Molecular Dynamic Investigation of the Interaction of Supported Affinity Ligands with Monoclonal Antibodies

ARTICLE *in* BIOTECHNOLOGY PROGRESS · JUNE 2008

Impact Factor: 2.15 · DOI: 10.1021/bp070469z · Source: PubMed

Molecular Dynamic Investigation of the Interaction of Supported Affinity Ligands with Monoclonal Antibodies

Laura Zamolo, Valentina Busini, Davide Moiani, Davide Moscatelli, and Carlo Cavallotti*

Dept. Chimica, Materiali e Ingegneria Chimica G. Natta, Politecnico di Milano, Via Mancinelli 7, 20131 Milano, Italy

Diagnostics and therapeutic treatments based on monoclonal antibodies have been attaining an increasing importance in the past decades, but their large scale employment requires the optimization of purification processes. To obtain this goal, research is focusing on affinity chromatography techniques and the development of new synthetic ligands. In this work we present a computational investigation aimed at obtaining some guidelines for the rational design of affinity ligands, through the study of their interactions with both monoclonal antibodies (modeled as the FC domain of human IgG) and a model support material (agarose). The study was carried out performing molecular dynamics simulations of the support-spacer-ligand-IgG complex in explicit water. Binding energies between IgG and two supported ligands, a disubstituted derivative of trichlorotriazine and a tetrameric peptide, were determined with the linear interaction energy and MM-GBSA approaches. A detailed study of the possible binding sites of the considered ligands was performed exploiting docking protocols and MD simulations. It was found that both ligands bind IgG in the same site as protein A, which is the hinge region between the CH2 and CH3 domains of IgG. However this site is not easily accessible and requires a high mobility of the ligands. The energetic analysis revealed that van der Waals and electrostatic energies of interaction of the triazine ligand with the support are significant and comparable to those with the protein, so that they limit its capability to reach the protein binding site. A similar result was found also for the tetrameric peptide, which is however able to circumvent the problem; for steric reasons only two of its arms can interact at the same time with the agarose support, thus leaving the remaining two available to bind the protein. These results indicate that the interaction between ligand and support material is an important parameter, which should be considered in the computational and experimental design of ligands for affinity chromatography.

1. Introduction

In the past decades monoclonal antibodies (MABs) and immunoglobulin G (IgG) in particular have been gaining an increasing importance in diagnostics and therapeutic treatments of acute diseases such as immunodeficiency, Alzheimer's syndrome and cancer (*1*−*3*). At present, several MABs (about 20) have been approved for sale by the U.S. Food and Drug Administration, and it is estimated that about 300 are being developed (*4*, *5*). In the past 3 years the value of the MABs market has doubled, passing from $ 10.3 billion in 2004 (*4*) to $ 20.6 billion in 2006, and it keeps growing at such a rate that it has been recently depicted as a new gold rush (*6*).

The increasing demand for these pharmaceuticals, reaching up to tons per year, has raised a number of issues for their large-scale production, from both the economic and technological point of view (*7*). The industry efforts to ensure that the manufacturing capacity could meet market requirements resulted in major advances in mammalian cell culture technology, enhancing its productivity to the gram per liter range (*8*), and in molecular engineering, allowing the reduction of MAB dosage by augmenting their effectiveness and their residence time in the body (*9*, *10*). Besides, a critical aspect in the production of MABs is their purity, which given their use for clinical purposes must reach yields of nearly 100%. Downstream processes, among which purification plays a key role, may represent up to 50−80% of the total production cost (*11*, *12*); these data evidence the pressing need for improvements in the purification steps.

Affinity chromatography (AC), based on the development of specific interactions between the antibody and a ligand, is one of the most employed methods for IgG purification. Protein A and protein G are among the most common affinity ligands used at present, thanks to their high binding capacity and selectivity; however, they present elevated costs of production, have leakage and contamination problems, and low resistance to sterilization (*13*−*15*). Thus, to improve AC performances and contain the costs, synthetic ligands are being researched by means of combinatorial chemistry and computer-aided molecular design (*16*−*20*). The properties required of these ligands are extremely demanding: they should guarantee most, if not all, of the selectivity of natural ligands and overcome their drawbacks in terms of manufacturing expense, leakage, and chemical and biological stability (*21*).

Usually the computational design of new ligands for proteins is performed neglecting the effect of a support on which the target molecule might be adsorbed. However, it is known that the support and the chemical composition of a spacer arm can affect the protein binding process. In a review concerning rational design of affinity ligands (*22*), Lowe gives emphasis to the fact that the affinity of a supported ligand for the complementary protein depends not only on its own character-

* To whom correspondence should be addressed. Phone: +39 02 2399 3176. Fax: +39 02 2399 3180. E-mail: carlo.cavallotti@polimi.it.

10.1021/bp070469z CCC: $40.75
Published on Web 05/02/2008

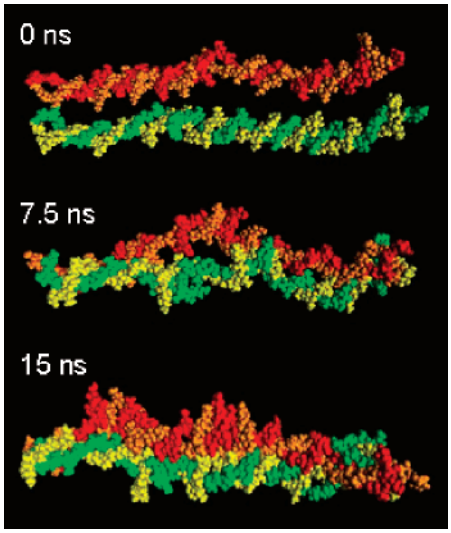

Figure 1. Snapshots of a 15 ns MD simulation performed for two 108-unit agarose double helixes.

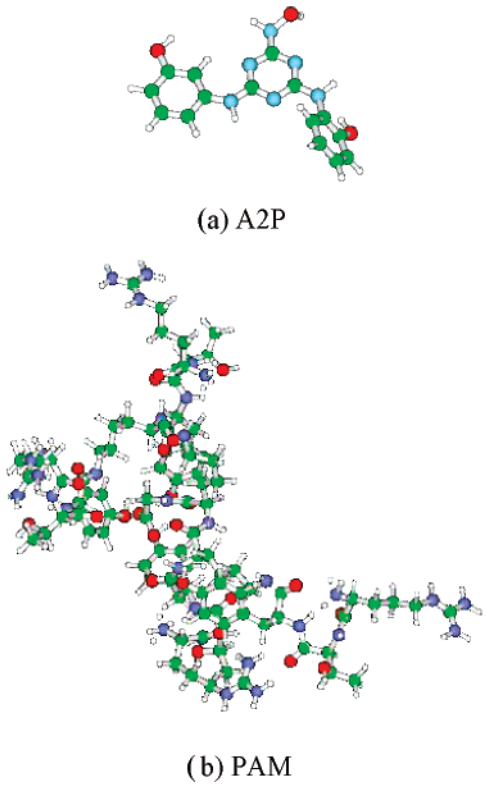

Figure 2. Structures of the (a) A2P and (b) PAM ([NH_2-(*R*)ARG-(*R*,*S*)THR-(*R*)TYR]$_4$-(*S*)LYS_2-(*S*)LYS-GLY) ligands considered in the simulations.

istics but also on the matrix activation and coupling chemistry. If the analysis of the system is restricted to the complex formed by protein and ligand, once the complete system is considered, the efforts of the rational design might be affected by unnoticed factors, such as the chemical, geometrical, and steric constraints imposed by the support. These considerations clearly indicate the need for a more detailed investigation of the supported system, aimed at extending the rational design to all of its components.

A first step in this direction is represented by the work of Zhang et al. (*23*), who studied, by means of molecular dynamics (MD), the behavior of a charged molecule (desmopressin) in an electrolytic solution and its adsorption on a charged surface. The simulations could describe the conformation of desmopressin in the bulk phase and upon adsorption explained the concentration overshoots experimentally observed, proved the importance of electrophoretic migration in the transport mechanism (due to the dominant electrostatic interactions), and made it possible to calculate the transport coefficient. The effect of adsorbed desmopressin on the subsequent adsorption of other molecules was evaluated, and the importance of considering explicit water when analyzing charged systems was underlined. Moreover, this study confirmed and improved a macroscopic continuum model previously developed, which had already provided useful indications for the design of purification systems of charged macromolecules, such as ion-exchange chromatography (*24*).

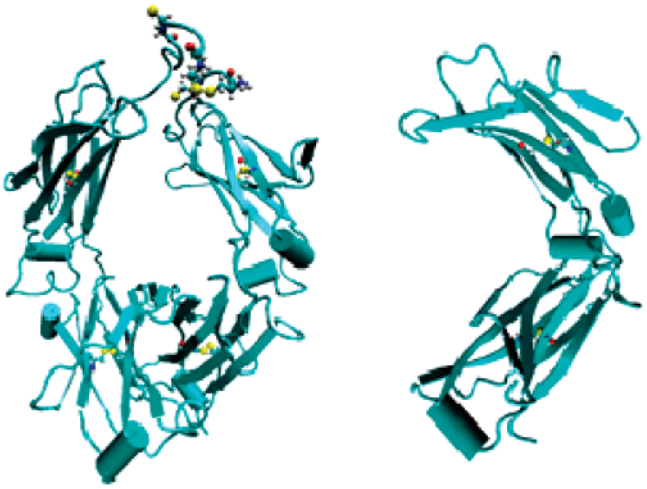

Figure 3. Model of the FC domain of IgG for A2P (left) and PAM (right): α-helixes are represented as cylinders, *β*-sheets as arrows; cysteine residues are fully displayed to highlight disulfide bridges.

Table 1. A2P System: Docking Energies (kcal/mol) of the Best Poses Evaluated with Different Search Boxes

pose	large box	small box
1	−8.79	−7.90
2	−8.57	−7.74
3	−8.23	−6.58
4	−8.20	−6.48
5	−8.12	−6.44
6	−7.54	−6.40

In a previous publication (*25*), we demonstrated that ligands bound to a support through spacers of different length and chemical composition can significantly interact with the support itself. Such interaction is influenced by the spacer physical and chemical properties and can lead to a conformational change of the system in which the ligand, instead of being uniformly solvated by water, can adsorb on the support. It was shown that the driving forces for this conformational change are van der Waals interactions between ligand and support. This is determined by the fact that ligands for monoclonal antibodies are known to interact mostly with a particular binding site of IgG, usually referred to as the "consensus binding site", which is characterized by a high conformational mobility and the capability to have hydrophobic interactions (*26*). Thus, in order to investigate whether the presence of a support can influence the ligand binding chemistry, MD simulations of the support-spacer-ligand-IgG complex were performed.

2. Theoretical Basis

The molecular structure used as model of the immobilized ligand can be decomposed into four parts: support, spacer, ligand, and protein. Support, spacer, and ligands are covalently

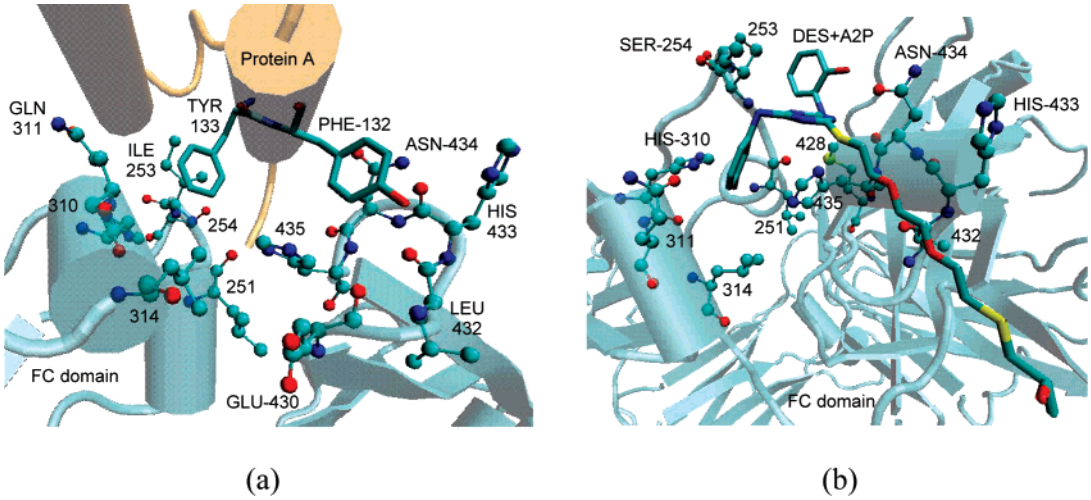

Figure 4. Comparison between (a) Protein A (crystallographic data) and (b) DES+A2P binding poses.

bonded and bind the protein through electrostatic, van der Waals, and hydrophobic forces. The support-spacer-ligand model here used was first introduced and discussed in a previous publication (*25*). The molecular structure used to represent agarose consists of two intertwined double helixes held stretched by restrains applied on terminal residues. The double helix coordinates were taken from the Protein Data Bank (PDB) (1AGA), while the entangled structure was obtained after a 30 ns MD simulation of two parallel agarose double helixes (Figure 1), containing 108 agarose residues each, solvated using explicit TIP3P water molecules and a solvent shell of 12 Å. After 15 ns the system converged to the structure reported in Figure 1, which was maintained for the successive 15 ns.

The agarose molecular model sketched in Figure 1 presents the advantage of being more stable and subject to lower deformations than the single double helix model; besides, the size of this system is comparable to that of the protein that we intend to simulate and significantly smaller than that of the agarose pores (typical diameters of 50−500 nm). This means that the curvature of the surface of an agarose pore due to its pseudocylindrical shape cannot be observed at the length scales here investigated and can thus safely be neglected.

The ligands considered in this study are two and differ in size and chemical properties. The first, A2P (Figure 2a), is a disubstituted phenolic derivative of trichlorotriazine designed by Prometic to bind selectively IgG (*19*), the interactions of which with an agarose surface were described in our previous publication (*25*). The second is a tetrameric peptide of formula [NH_2-(*R*)ARG-(*R*,*S*)THR-(*R*)TYR)$_4$-(*S*)LYS$_2$-(*S*)LYS-GLY] discovered by Xeptagen by screening multimeric combinatorial libraries (Figure 2b) (*17*). We will refer to this ligand in the following as PAM. The choice of these two ligands is significant as both have been designed experimentally with the aim of mimicking protein A interactions with IgG, though PAM is significantly more complex than A2P, both in terms of structure and internal conformational mobility. Moreover, the experimental data proved that these molecules maintain their binding capability also when immobilized on a support and in particular on agarose or agarose-based gels, thus explaining the choice of the support model for our present and previous works (*25*).

The spacers used to connect through covalent bonds the ligands to agarose are CH_2-CHOH-CH_2-S-$(CH_2)_2$-O-$(CH_2)_2$-O-$(CH_2)_2$-S (DES) for A2P and CHOH-$(CH_2)_4$-CHOH (SX4) for PAM (*27*).

The structure adopted as the IgG molecular model for the A2P−IgG complex consists of the full fragment crystallizable (FC) region, which is composed of two identical domains (two CH2-CH3 chains), connected at the top by a cysteine bond (Figure 3, left).

The FC fragment coordinates were taken from the PDB crystal structure 1HZH (human IgG), which also included the coordinates of the two FAB domains of the protein. FAB domains were not considered in the simulations as both ligands were designed to bind the FC domain of MABs, which is thus expected to be the part of the antibody that mostly interacts with the supported ligand. In particular PAM was found by screening combinatorial libraries in search of a molecule that might disrupt the interaction of protein A with IgG, which gives indirect evidence that the binding site of PAM is the same of protein A, i.e., the consensus binding site (*17*, *28*). Though the location of the binding site for both ligands is most likely on the FC domain, it cannot be excluded a priori that the FAB domain might interact with the agarose surface. It is however likely that this second interaction would be nonspecific, as it is improbable for steric reasons that a protein might form more than one specific bond with a functionalized surface. Neglecting the FAB domain has the significant advantage of reducing considerably the size of the system and thus the computational time. The aminoacidic sequence was cut in correspondence to the cysteine residues linking the two CH2 subdomains of the antibody. The disulfide bond proved fundamental to preserve the structure of the immunoglobulin unaltered; MD simulations (8 ns) of the FC fragment without this bond, in fact, showed that the two CH2-CH3 chains would drift apart. At the opposite ends of the FC fragment, the CH3 domains are kept together by hydrophobic interactions. The PDB file was further modified as follows:

- hydrogen atoms were added considering HIS residues not protonated, as this is the active form of histidines at the pH at which chromatographic separations of IgG is usually performed (pH = 7.6 for A2P (*19*); pH = 6.8 for PAM (*17*)).
- CYS residues were treated as CYX (defined in Amber force field Parm94 (*29*), which was used in this work) to take account of the formation of disulfide bonds between cysteines.

After that, a MD simulation of 2 ns was performed in explicit water to allow the FC structure to relax from its crystallographic pose.

For the Xeptagen ligand a different model was used to describe IgG (Figure 3, right). The initial structure was based on crystallographic data relative to the FC domain bound to one of the four arms of the ligand (*30*). In these data some of the terminal residues of the FC fragment, among which the

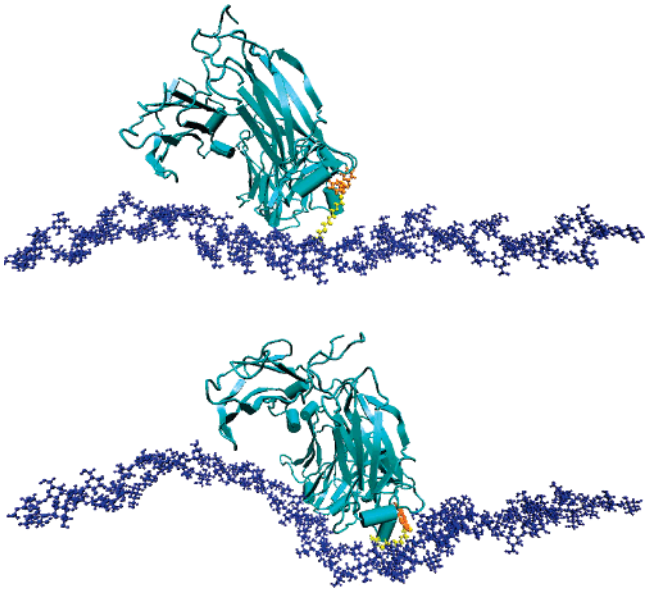

Figure 5. Initial and final snapshot of a 5 ns simulation using as molecular model the full FC domain of IgG, A2P, DES, one agarose double helix, and 10,430 water molecules.

cysteines involved in the S−S bond, were not included; thus, due to the difficulty to reconstruct the 1HZH protein without altering considerably its structure, it was decided to consider only half FC domain. This choice, which implies a significant decrease of the size of the system, is in part justified by the additional rigidity that the PAM−IgG complex has with respect to the A2P−IgG system. This is determined by the larger size of PAM and by the fact that it interacts with a significant portion of IgG in the consensus binding site region, which is the one known to suffer from significant conformational changes. As in the previous case, the X-ray structure was completed with hydrogens and CYX residues were connected to reproduce the disulfide bridges inside the CH2 and CH3 domains. Residues of the FC sequence are referred to in the following according to Deisenhofer's numeration of the IgG−protein A complex (PDB id 1FC2, ref 31).

The conformational evolution of the IgG-ligand-spacer-support system was investigated using MD simulations. This molecular modeling method is based on the integration of Newton's second law, through which, knowing the force F_i acting on each atom i of the system, it is possible to determine its acceleration a_i (and thus its position r_i and velocity v_i) as it varies with time. F_i is usually expressed as the gradient of the potential energy of the system, E, which is defined by means of a suitable force field.

In the present work, MD simulations were performed using the force fields supplied in the Amber suite (*32*), whose description of E is composed of five terms: bond stretching, bond bending, bond twisting, Van der Waals, and electrostatic interactions (*29*). The Glycam 04 (*33*−*35*) force field, modified as described in ref 25 to include the 3,6-anhydro-galactose residue, was used to describe the agarose support, while the Parm94 force field (*29*) was chosen for spacers, ligands, and the protein, as its parameters are consistent with those of Glycam. For ligands and spacers new parameters were evaluated; in particular, for the PAM molecule some of the aminoacids defined in the Amber library needed to be modified: new LYX, TYX, and XRG residues were defined to reproduce PAM inner bonding between LYS side chain amine group and TYR, and between ARG and SX4. These parameters were derived from quantum chemistry calculations (as in ref 25),

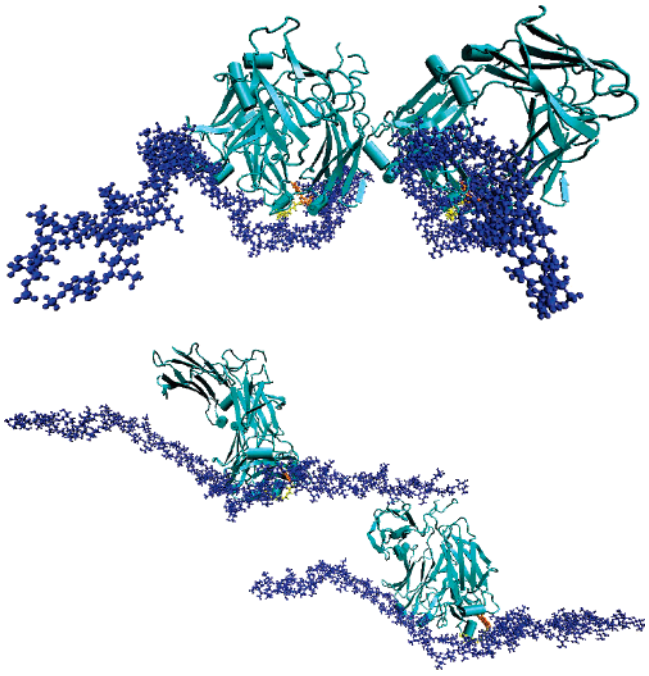

Figure 6. Representation of two periodic cells containing the investigated molecular system: full Fc domain of IgG, A2P, DES, one agarose double helix, and 10,430 water molecules.

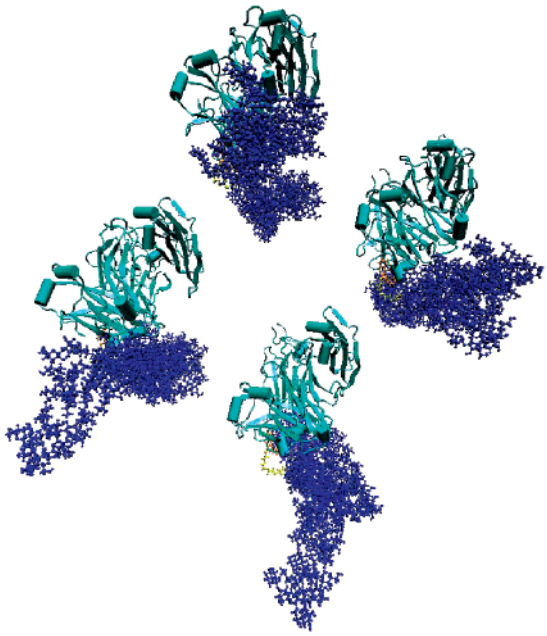

Figure 7. Representation of two periodic cells containing the investigated molecular system: full Fc domain of IgG, A2P, DES, two agarose double helix, and 25,750 water molecules.

consistently with the Parm94 force field: first the geometry of each molecule was optimized using density functional theory at the B3LYP/6-31g(d,p) level (*36*−*39*); successively the atom charges were computed via the RESP formalism (*40*). This method consists of a two-step fitting of the charges to reproduce the electrostatic potential (ESP) of the molecule; the fitting procedure introduces restraints (R-ESP) on non-hydrogen charges to reduce the overall magnitude of computed charges.

The X-ray structures of IgG, modified as specified above, were used for the simulations. The ligand−protein complex was bound to agarose and successively solvated in an explicit water shell of 20 Å, which corresponds to about 25,000 water molecules. All simulations were performed using a dielectric

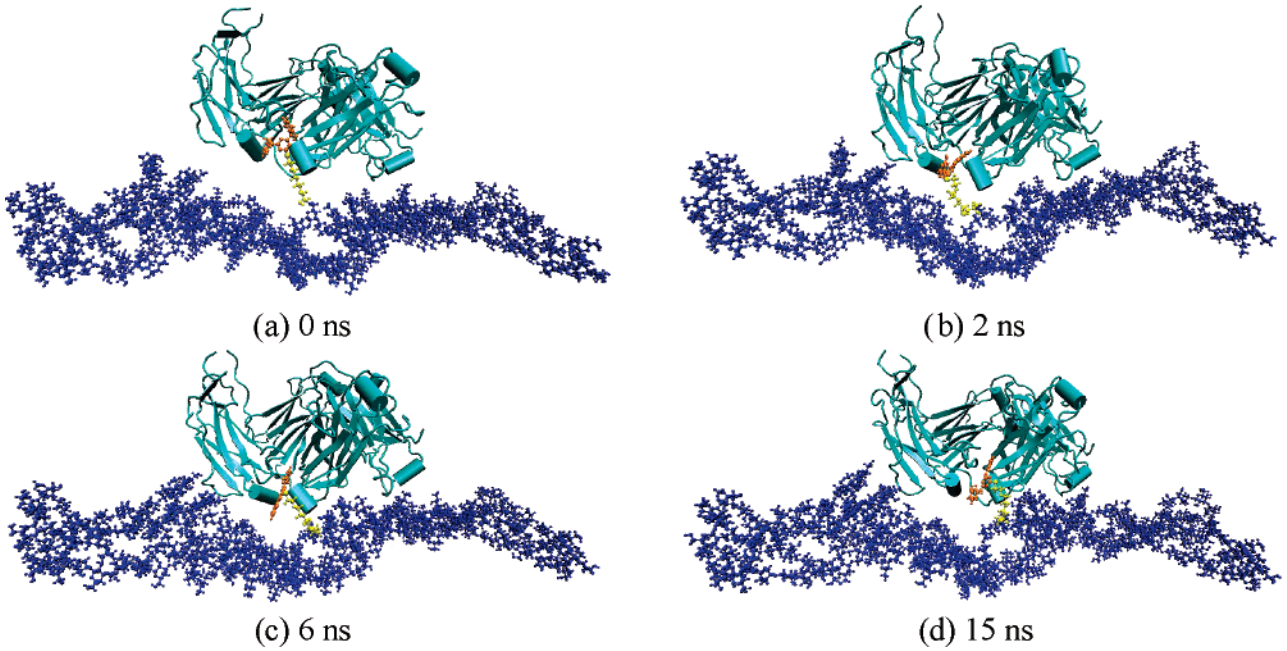

Figure 8. Snapshots of the MD simulation of the full FC domain of IgG bound to A2P immobilized on agarose.

constant of 1 and a nonbonded cutoff of 10 Å for all interactions. Periodic boundary conditions were applied to the system, and long-range electrostatic interactions were evaluated using the Particle Mesh Ewald method (*41*): thus, the system is divided in unit cells of equal size and a particle within each unit cell interacts with all the other particles in the same cell as well with all their periodic images in the neighboring cells.

MD simulations were performed following a five-step protocol, analogous to that considered in our previous paper (*25*). The first step consisted in a 2000 cycles minimization to remove any possible unfavorable contact between solvent and solute. The first 1000 cycles of the minimization were performed with the steepest descent method, followed by 1000 cycles with the conjugate gradient method. In this step the complex is restrained with a harmonic potential of the form $k(\Delta x)^2$, where Δx is the displacement and k the force constant ($k = 500$ kcal/mol/Å^2). Subsequently, a 3500 cycles minimization (1500 steps of steepest descent and 2000 steps of conjugate gradient method) without restraints was performed. The next stage consisted of a simulated annealing of 20 ps at constant volume to raise the temperature of the system from 0 to 300 K; in this phase, a weak restraint was imposed on the complex ($k = 10$ kcal/mol/Å^2) to avoid wild structural fluctuations. Finally a 100 ps run at constant pressure (equilibration phase) was carried out to allow the water density to relax, followed by the production MD run of a standard period of 15 ns. These last two steps were performed at 300 K and constant atmospheric pressure; restraints were applied only on agarose ends ($k = 10$ kcal/mol/Å^2) to limit the mobility of its chains.

The SHAKE algorithm was used for all the covalent bonds involving hydrogen, in order to remove the bond stretching freedom, which is the fastest motion; this allowed the use of a time step of 2.0 fs (*42*).

Binding free energies between protein and supported ligands were determined using both the MM-GBSA/PBSA and the linear interaction energy (LIE) protocols. In the former case, the $\Delta G_{binding}$ was calculated as

$$\langle \Delta G \rangle = \langle \Delta E_{MM} \rangle + \langle \Delta \Delta G_{Sol} \rangle - T\Delta S_{Gas} \qquad (1)$$

where ΔE_{MM} is molecular energy change in the gas phase for the reaction of dissociation of the complex and is determined by the sum of three contributions:

$$\langle \Delta E_{MM} \rangle = \langle \Delta E_{Int} \rangle + \langle \Delta E_{El} \rangle + \langle \Delta E_{VdW} \rangle \qquad (2)$$

which correspond to changes in internal energy (composed of bond stretching, angular deformation, and torsional energy), electrostatic energy (expressed as Coulomb interaction between point charges), and Van der Waals energy (expressed through Lennard Jones potentials). $\Delta\Delta G_{Sol}$ is the difference between the solvation free energy of the complex ($\Delta\Delta G_{Sol}$LP) and that of the ligand ($\Delta\Delta G_{Sol}$L) and of IgG ($\Delta\Delta G_{Sol}$P). Each of these terms consists of two contributions: the first one accounts for the electrostatic component and can be calculated with a suitable solvation model, such as that provided by the Poisson−Boltzmann (PB) approach. This model represents the solvent as a dielectric continuum rather then as individual molecules and describes the electrostatic environment of a solute in a solvent containing ions through the PB equation (*43*) or, given the difficulty of solving efficiently the PB equation, an approximate solution. Among the approximate solutions of the PB equations, the Generalized Born (GB) approach, based on an analytical formula, has been widely employed (*44*). The second term refers to the apolar contribution and was evaluated as a linear function of the solvent-accessible surface area (SASA) (*45*, *46*). MM-PBSA and MM-GBSA calculations were performed for the supported ligands in complex with IgG. Unfortunately the PB results for the A2P system were not converged within the grid used for the integration (2 grids/Å), and systematically increasing the grid, though decreasing the fluctuations of the computed energy, did not resolve the problem in a definitive way. Finally, $T\Delta S_{Gas}$ is the entropy difference between complex, ligand, and protein and was calculated considering only the rotational and translation contributions, which were determined through statistical thermodynamics neglecting the vibrational term. Medium energies were averaged on time spans of 1 ns.

Alternatively to the MM-PBSA method and to complement its results, free binding energies were computed using the linear

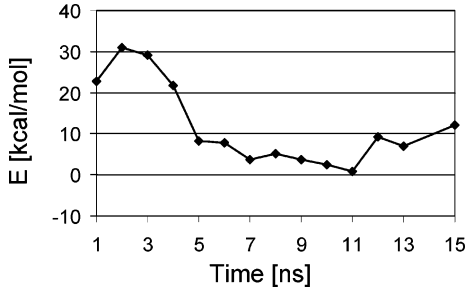

Figure 9. A2P complex: binding energies ($E = E_{MM} + \Delta G_{solvGB} - T\Delta S_{gas}$) evaluated with the MM-GBSA protocol and averaged on time spans of 1 ns.

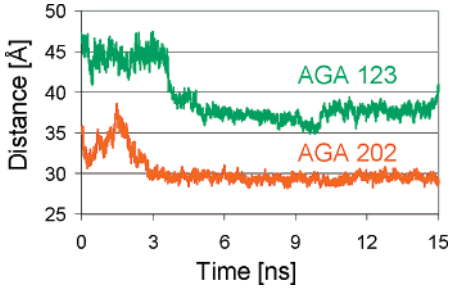

Figure 10. A2P system: time evolution of the distance between the IgG FC center of mass and two agarose key residues.

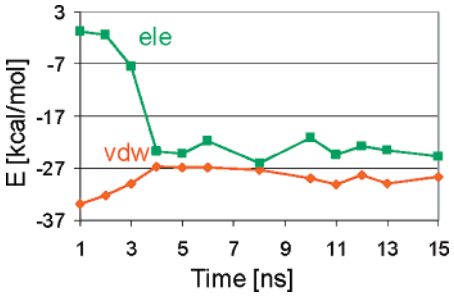

Figure 11. Variation of van der Waals (orange line) and electrostatic (green line) interaction energies of A2P and DES with the surrounding environment (water + protein) between the free and the bound state, averaged on time spans of 1 ns.

interaction energy (LIE) approach (*47*). This method evaluates the binding free energy by comparing the interactions the ligand develops with its surrounding environment in its "bound" (i.e., the ligand complexed with the protein) and its "free" state (i.e., the ligand not bound to its receptor). The polar and nonpolar contributions to ΔG are treated separately and are considered to scale linearly with electrostatic (V^{ele}) and van der Waals (V^{vdw}) interaction energies, respectively (eq 3). The linear scaling of the electrostatic term derives from the linear response approximation, which describes the response of polar solutions to changes in electric fields (*48*), while that of the nonpolar term results from the observation that both solvation free energies of nonpolar compounds and van der Waals energies scale linearly with solute size measures, such as its accessible surface area (*49*, *50*).

$$\langle \Delta G \rangle = \alpha(\langle V^{vdw}_{bound} \rangle - \langle V^{vdw}_{free} \rangle) + \beta(\langle V^{ele}_{bound} \rangle - \langle V^{ele}_{free} \rangle) \quad (3)$$

In our system, the surrounding environment of the bound ligand includes the solvent, the antibody, and agarose, while in the free state it consists of agarose and water molecules. Thus, two different MD simulations were performed for each ligand: the first for the agarose-spacer-ligand-FC complex (15 ns) and the second for the supported ligand alone (agarose-spacer-ligand). In the latter case, the simulation protocol was analogous to the one used for the complex, but a shorter time span (3 ns) was considered, as this was sufficient to stabilize the system.

Interaction energies were determined with the Anal. program of the Amber 8 computational suite, and their medium values for the bound state were averaged on a time span of 1 ns, while for the free state they were averaged on the last nanosecond of the simulation. Following LIE theory, the protein-supported ligand free binding energy was computed from the electrostatic and van der Waals energy changes between free and bound state using as weight factors α and β the recommended values (*47*) of 0.18 and 0.5.

MD and ab initio simulations were performed using the Amber 8 computational suite (*32*) and Gaussian 03 (*51*), respectively; all structures reported in this work were produced using Molden 4.4 (*52*) and VMD 1.8.2 (*53*).

3. Results and Discussion

In this section we report and analyze the results of the MD study of the interaction between IgG and supported ligands. In section 3.1 we describe how we determined the binding structure of ligand and IgG that were used as starting point for the simulations. Then the influence of several parameters, such as the dimension of the solvation shell and the size of the support model, on the conformational evolution of the solvated protein complexes are reported in section 3.2. Finally, in sections 3.3 and 3.4 the results of the MD simulations are discussed.

3.1. Protein−Ligand Binding Structures. Docking simulations were performed using Autodock 3.0 (*54*) to obtain first guess binding structures of the [A2P + DES]−IgG complex. The ligand was defined as the sum of A2P and spacer, covalently connected. This choice was taken in part because the explicit consideration of the spacer restricts the binding conformational space investigated to only those poses consistent with the presence of a long spacer arm fully or partially stretched and in part by the simplification this approach gives in connecting the ligand to the agarose support easily when defining the starting geometry for the MD simulations of the complete system. For this purpose the spacer was defined as rigid (none of its bonds were kept rotatable), while A2P was left free to rotate around the sp^3 bonds. Docking was carried out holding the receptor (i.e., the FC domain) fixed and letting the ligand move over its surface. Two search boxes of different size were considered, both centered on the *consensus binding site* and large enough to allow the ligand to rotate freely and to investigate the possible existence of different binding sites. The larger box ($80 \times 80 \times 110$ grid points with a spacing of 0.375 Å) enclosed about one-third of the half FC domain, while the smaller one consisted of a $60 \times 60 \times 60$ grid. For each search set about 30 poses were evaluated using a Lamarckian Genetic Algorithm (*54*), and among these the minimum energy one was chosen if it could satisfy the following criteria:

- the ligand cannot interact with the inner surface of the protein and the spacer needs to be turned toward the solvent to take account of the steric hindrance of the agarose support;
- poses in which A2P is nearby the consensus binding site were preferred, since this is known to be the favorite interaction zone.

The docking energies of the best poses are reported in Table 1; it can be noted that the simulation with the larger search box gave higher energy values. However in these poses the DES spacer is oriented toward the protein surface; for this reason

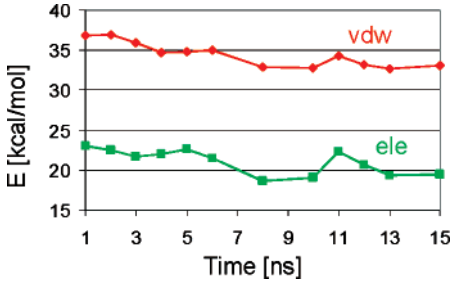

Figure 12. Variation of van der Waals (orange line) and electrostatic (green line) interaction energies of A2P and DES with agarose between the free and the bound state, averaged on time spans of 1 ns.

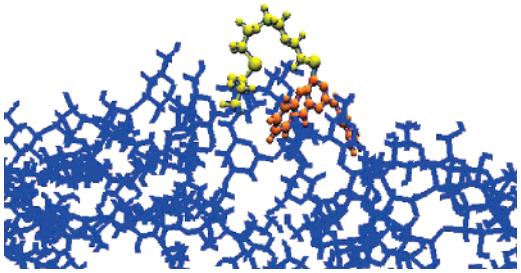

Figure 13. Final conformation of the AGA-DES-A2P system after 3 ns.

they were excluded and the first pose of the smaller box simulation was selected for the MD runs (Figure 4 b).

The A2P molecule was designed to mimic the specific interactions of protein A with IgG and in particular of its PHE 132 and TYR 133 residues. The success of such intent is, at least computationally, confirmed by the results of the docking procedure, which predicted structure is compared with that of protein A in Figure 4. In fact, it can be observed that A2P binds preferentially with the same key IgG residues with which protein A interacts (*18*, *31*). In particular the docking pose shows that one of the two hydroxyphenyl groups of the synthetic ligand interacts with HIS 310, GLN 311, LEU 314 and MET 428, ASN 434, HIS 435, while the other one with ILE 253 and SER 254 of the FC domain (Figure 4). These are the same residues involved in the interaction of the PHE 132 and TYR 133 residues of protein A with IgG.

As for the PAM ligand, the initial structure of its complex with IgG was obtained by crystallographic data (*30*). Unfortunately only a part of the binding structure of PAM could be resolved and specifically that consisting of a full arm (ARG-THR-TYR), two sequential LYS residues, and the terminal GLY. The strategy we adopted to reproduce the full PAM-IgG binding structure consisted then of adding the residual three arms and LYS residues to the X-ray structure in an extended conformation, thus avoiding the imposition of any pre-computed geometry. The complex thus obtained was then relaxed through a MD simulation of 2 ns maintaining the X-ray part of PAM frozen. This allowed to find for the experimentally undetermined part of the Pam-IgG complex an energetically relaxed structure which is consistent with the X-ray structure. Successive MD simulations performed in the absence of restraints confirmed the stability of the structure so determined, which did not change significantly from that determined through the restrained MD simulations.

3.2. Optimization of the Molecular Model. A preliminary analysis was performed to investigate the influence of several parameters on the MD simulations. In particular we examined

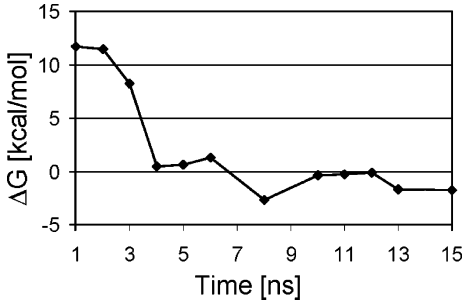

Figure 14. Free binding energies between the immobilized A2P ligand and IgG evaluated with the LIE protocol and averaged on time spans of 1 ns.

Table 2. PAM Residues Involved in H Bonds with Agarose or FC or Intramolecular H Bonds

PAM Residues Interacting with Agarose	
LYS 213, GLY 214, THR 216, THR 220, ARG 222, THR 223, TYR 224	
Mutually Interacting PAM (left) and FC (right) Residues	
ARG 209	THR 250, ARG 255
THR 210	GLN 311
TYR 211	ASP 280, LYS 317
ARG 215	GLU 318
THR 216, TYR 217	ASP 315
ARG 219	ALA 431
Intramolecular PAM Hydrogen Bonds	
GLY 214	ARG 222
THR 216	ARG 215, LYS 218
TYR 217	ARG 219, THR 221
THR 223	LYS 218, THR 221

the effects of the dimension of the solvation shell and of the size of the agarose model (one or two double helixes). These test simulations were performed for the A2P system.

The first molecular model considered comprised a full FC domain, the A2P ligand, the DES spacer, one agarose double helix held stretched by terminal restraints, and a 12 Å solvation shell (about 10,000 water molecules). The initial and final snapshots of a 5 ns simulation are sketched in Figure 5.

The simulations evidenced a significant distortion of the agarose support, which took place despite the application of restraints, probably because of the interaction with the protein. Moreover, the size of the cell is not sufficient to avoid the interaction of part of the FC domain of a cell either with its periodic image or with the agarose double chain in an adjacent cell; this is evidenced in Figure 6, where two neighboring periodic cells are sketched.

To solve these problems, the solvation shell was increased from 12 to 20 Å, which corresponded to an increase of the water molecules from 10,430 to 25,750, and the agarose single chain was substituted with the double chain model. The size of the simulation box ($180 \times 152 \times 115$ Å^3) guarantees the absence of interactions between the periodic cells, as shown clearly in Figure 7.

The substitution of the single chain with the double chain model decreases significantly the mobility of agarose, as the rms fluctuation with respect to its backbone drops from 10 Å in the case of the single chain to about 4 Å for the double chain. The double chain agarose structural model here proposed is based on the available literature evidence and in particular on the seminal works of Arnott et al. (*55*), who initially proposed that agarose is formed by bundles of double helixes, left handed, with a helix pitch of 26 Å, and on the successive works of Ramzi et al. (*56*, *57*) and, more recently, of Xiong et al. (*58*), who

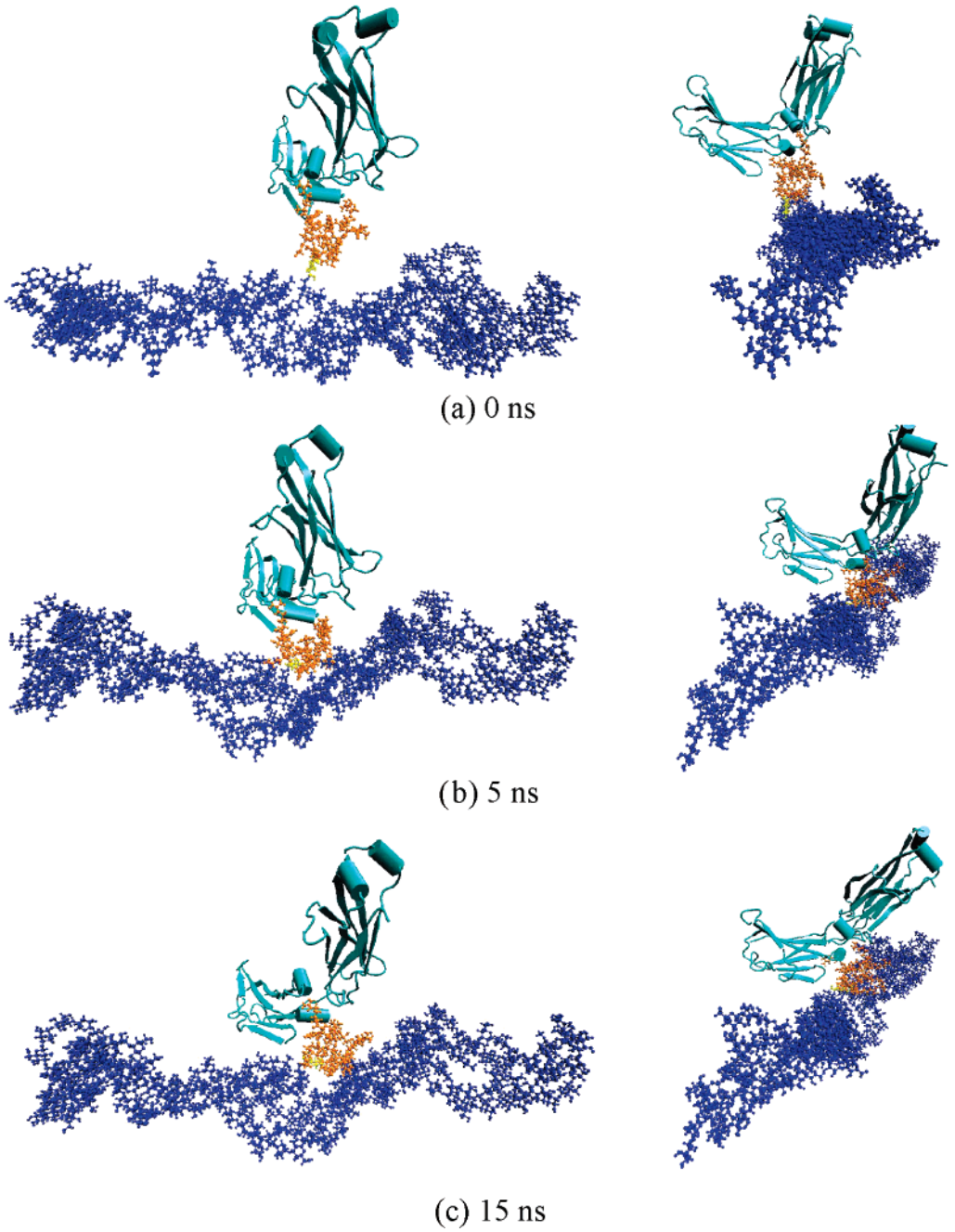

Figure 15. Time evolution of the PAM system: frontal (left) and lateral (right) view of the complex at different simulation times.

suggested that agarose should be thought of as a random assembly of straight fibers. Clearly, a fiber will be formed by more than a set of two double helixes. To investigate which might be the effect of the presence of more than two double helixes, we have previously performed simulations also with a system comprising three double helixes (*25*). The results indicated that agarose tends to form structures in which not more than two double helixes are coupled at the same time, thus suggesting that a double helix model might be sufficient to describe the local agarose surface properties.

On the basis of this analysis we concluded that the optimal molecular model structure to be adopted in the MD simulations consists of the full FC domain of IgG, the ligand, the spacer, the agarose model containing two double helixes, and about 25,000 water molecules.

3.3. MD Simulations and Energetic Analysis of the Interaction of IgG with Supported A2P. The conformational evolution of the FC domain of IgG bound to A2P supported on agarose was investigated through a 15 ns molecular dynamic simulations. Four structures representative of the system at different times are reported in Figure 8.

During the simulations the same IgG−ligand binding site is maintained, which indicates that the bond between A2P and IgG is stable. The most evident conformational change is the progressive approach of the FC fragment to the agarose helixes. This transformation of the system takes place in the first nanoseconds and causes a distortion of the DES spacer, initially straight. Agarose helixes display as well a partial reorganization, despite the restraints, which can reasonably be attributed to the steric hindrance and the interactions, both polar and hydrophobic, with IgG. As a result of the approach of IgG toward agarose, several hydrogen bonds are formed between some agarose hydroxyl groups and the protein; the FC groups involved in these bonds are both carbonyl groups of its backbone and the

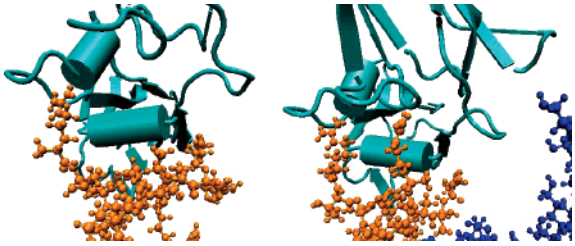

Figure 16. PAM system: initial pose (left) and structure after 5 ns (right).

side chains of residues containing carboxyl or hydroxyl groups (GLU 283, GLU 345, THR 140), -$CONH_2$ groups (ASN 142) and -NH_3^+ groups (LYS 317). The extent of the interaction of some key protein and agarose residues was determined by calculating the change of van der Waals and electrostatic energy of interaction with the environment between the beginning of the simulation, when the protein and agarose are sufficiently distant so that no specific interaction are possible, and the end of the simulations. The calculated energies were averaged on a time span of 1 ns. It was found that the VdW and electrostatic energy of interactions of VAL 282 with the environment change by −2.85 and +3.41 kcal/mol, respectively, while that of two agarose residues, AGA 123 and AGA 202, change by −3.11 and +4.24 and by −5.53 and +3.44 kcal/mol, respectively. This indicates that some VdW interactions are formed between IgG and agarose between the start and the end of the simulation but that these interactions energies are counterbalanced by the loss of electrostatic energies of interaction with the environment of similar magnitude.

The results of MM-GBSA calculations, averaged on a time span of 1 ns and corrected with the gas-phase entropic term (only rotational and translation terms, about −33 kcal/mol), are reported in Figure 9. It can be noted that the entropic contribution leads in all cases to positive free binding energies. Though this seems to indicate that the complex is not thermodynamically stable, it must however be mentioned that, in our experience for these systems, MM-GBSA values energies are usually under-binding with respect to the more accurate MM-PBSA values. The gas-phase vibrational entropy contribution was not included in the evaluation of the MM-GBSA interaction energy. The motivation is two-fold: first it is difficult to estimate it reliably because of the large conformational space sampling that is necessary and then because, given the low mobility of the ligands both when in complex with the protein and when the protein is absent, we do not expect it to play a significant role.

Despite the uncertainty about the free binding energy absolute value, the qualitative trend of the results reported in Figure 9 is likely to be correct. It can be noted that the binding energy presents a maximum value in the first nanoseconds of simulation; after about 5 ns the system stabilizes and its energy fluctuates around a mean value. This stabilization is due to the reorganization of the agarose structure determined by the establishment of interactions between protein and support, as can be observed by comparing the calculated free binding energy change with the complex macroscopic re-organization. To quantify the degree of the protein displacement, the distance between its center of mass and two agarose key residues (123 and 202 according to our numbering scheme) was calculated and is reported in Figure 10; it can be observed that the distance is maximum for the initial structure of the complex and then decreases of about 5−7 Å in the first 3 ns of the simulation.

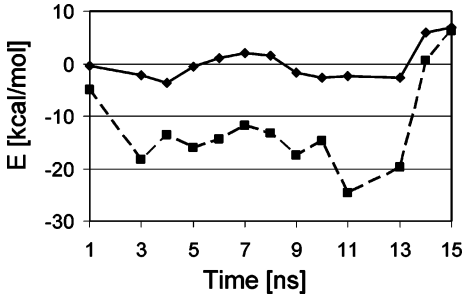

Figure 17. PAM system: free binding energies evaluated with the MM-GBSA (solid line) and MM-PBSA (dashed line) protocols.

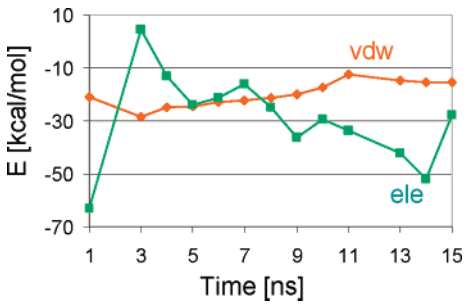

Figure 18. Variation of van der Waals (orange line) and electrostatic (green line) interaction energies of the SX4−PAM pair with the surrounding environment (water + protein) computed averaging energies on time spans of 1 ns.

Interestingly, toward the end of the simulation the distance between agarose residue 123 and the IgG FC center of mass slightly increases (about 2 Å); this might indicate a rearrangement in the conformation of some agarose residues closer to the protein, which might explain the increase of the energy of the system in the last 4 ns (Figure 9).

The differences between van der Waals and electrostatic interaction energies of the A2P−spacer complex with water and the FC domain in the bound state and of the A2P−spacer complex with the solvent in the free state (i.e., when the protein is not present) are reported in Figure 11. It can be noted that the interaction energy is more determined by hydrophobic than electrostatic forces. This was expected, as IgG is known to develop mainly hydrophobic interactions with its ligands. Moreover, while the former contribution displays almost a constant value, the latter shows a decreasing trend, which mirrors the $\Delta G_{binding}$ evolution during the simulation and indicates the increasing importance of electrostatic interactions in the stabilization of the system.

van der Waals and electrostatic energy changes between the free and the bound state of the A2P−spacer complex with the agarose support are sketched in Figure 12. The high positive values calculated indicate that strong interactions (mainly hydrophobic) are established between A2P and agarose in the "free state" (i.e., supported on agarose but not bound to the FC domain), which are lost when the complex with the protein is formed. In fact, in the absence of the protein the ligand lays on agarose instead of being fully solvated (Figure 13 and ref 25) and thus, in order to form the complex with IgG, the desorption of A2P from the support has to be paid energetically.

The energy of interaction between the protein and the A2P-spacer pair can be obtained adding the data reported in Figure 11 to those of Figure 12. These $\Delta V_{free \rightarrow bound}$ data can be used to evaluate the protein free binding energy using the LIE protocol as described in the method section. The trend of the

free binding energy so determined (Figure 14), showing a high initial value followed by a stabilization of the system at about −2 kcal/mol, confirms the qualitative indication provided by the MM-GBSA analysis and gives in addition some very important quantitative information. In fact, though A2P has been designed with the aim of having a high affinity for IgG, its predicted free binding energy is very small. This is because the high electrostatic and VdW energies of interaction calculated for the A2P ligand with IgG (Figure 11) are compensated by the energy necessary to break the interactions of the ligand with the agarose surface (Figure 12). This might give rise to several problems, including the formation of nonselective bonds with alternative protein binding sites, which do not require that A2P detaches from the agarose surface and might therefore be more easily reached than the consensus binding site. A second more general conclusion is that the interaction between ligand and support can influence significantly the protein binding process and should thus be considered in the computational and experimental design of ligands for affinity chromatography.

3.4. MD Simulations and Energetic Analysis of the Interaction of IgG with PAM. The conformational evolution of the FC domain of IgG bound to PAM supported on agarose was studied for the same time interval of 15 ns adopted to investigate the A2P system. With respect to A2P, PAM is a large and complex molecule, formed by four arms containing three aminoacidic residues each; this prevents the IgG FC from interacting with the agarose chains, as the ligand is constantly interposed between them. Nevertheless, as the system evolves, the FC domain moves toward the support with respect to the initial pose, in which SX4 is fully outstretched; contextually, PAM rearranges its conformation and establishes some interactions with agarose (Figure 15).

Thanks to the higher rigidity of the PAM−IgG complex with respect to the A2P system, the half FC model here considered proves stable for most of the simulation; however, it presents a major distortion after about 13 ns, when the CH2 and CH3 domains of the FC fragment start aligning (Figure 15 c).

The analysis of the first 13 ns shows that PAM is involved in an extensive network of both hydrophobic interactions and H bonds with the protein and the support and between its own residues (Table 2). As was found for the A2P complex, these interactions may involve both the backbone carboxyl groups and the side chains of the protein residues.

It is interesting to observe that in the time span investigated a new interaction between PAM and FC, which is not present in the initial conformation, is developed as one of the arms of the ligand moves to interact with four protein residues (from ALA-431 to HIS 435, Figure 16). This seems to indicate that the same FC residues are involved in the interaction with PAM as with protein A and A2P. However this interaction proves stable for just the first 7−8 ns of the simulation, after which the PAM arm responsible for it starts drifting away to interact with other parts of the ligand or solvent molecules.

The results of MM-GBSA and MM-PBSA calculations for the PAM system, corrected with the gas-phase rotational and translational entropic terms and averaged over a time span of 1 ns, are reported in Figure 17. The free binding energy calculated using the MM-GBSA approach is rather flat for the first 13 ns, presenting only minor fluctuations. On the contrary, the more accurate MM-PBSA results show a trend similar to that found for the A2P system, displaying an initial energy decrease followed by fluctuations around a mean value. It is interesting to observe that both GB and PB calculations report a significant energy increase in the last 2 ns of the simulations, when the half FC chain starts straightening.

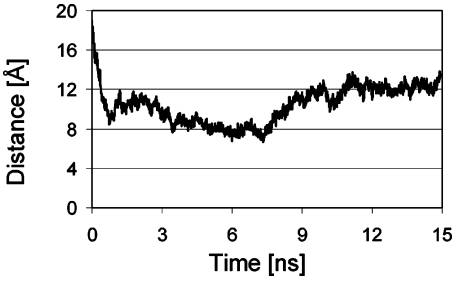

Figure 19. Time evolution of the distance between PAM and agarose centers of mass.

The variation of van der Waals and electrostatic energies of interaction with the environment, computed neglecting the interaction with agarose, displayed separately in Figure 20, are sketched in Figure 18. Contrary to the A2P system, it can be noted that the extent of electrostatic and van der Waals interactions between ligand and protein is comparable.

It is interesting to observe that by the first nanosecond the protein−ligand electrostatic interaction energy presents its minimum value; successively it rises to a maximum and stabilizes to a constant value. This might in part be explained by the fact that, in the initial structure of the complex, PAM does not interact with agarose. As the PAM−FC complex evolves, however, the ligand approaches the support, starts interacting with it and partially looses its solvation and thus its initial stability: the system needs time to find a new stable conformation. The distance between the PAM and agarose centers of mass decreases from an initial value of about 18 Å to 8 Å and after 9 ns reaches a mean value of about 12 Å (Figure 19).

The evaluation of the interactions between ligand and support confirms this interpretation. The electrostatic and van der Waals $\Delta V_{\text{free}\rightarrow\text{bound}}$ data reported in Figure 20 indicate that the interactions between PAM and agarose (mainly electrostatic) are minimum in the initial conformation of the complex and then increase as the system evolves.

The total interaction energy between the immobilized PAM ligand and IgG can be computed summing the data of Figures 18 and 20. The free binding energy can then be determined using the LIE protocol. The results, reported in Figure 21, show that the LIE free binding energy is slightly negative, with an average value of −4 kcal/mol. The contributions to the protein binding energy are significantly different from those observed for A2P. Electrostatic energy contributes very slightly to the bond strength, as the interaction energy between PAM and IgG is almost completely counterbalanced by that necessary to detach PAM from agarose, so that most of the protein−ligand interaction energy is given by VdW forces. The main difference between PAM and A2P is in the higher conformational mobility of the peptide ligand, whose four arms are only partly involved in the interaction with the substrate (not more than two arms at the same time), so that the ligand has always at least two arms free to interact with the protein. As will be shown in a successive work (*59*), PAM is able to bind IgG selectively by forming a contemporary interaction with two of its arms, one of which binds IgG in a specific site, while the other forms ionic interactions with charged protein residues. The fact that the interaction energy is mainly hydrophobic does not mean that no hydrophilic interactions, such as hydrogen bonds, are

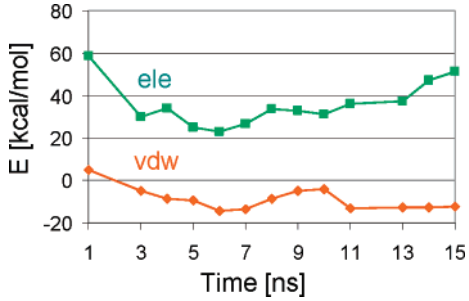

Figure 20. Variation of van der Waals (orange line) and electrostatic (green line) interaction energies of the SX4−PAM pair with agarose between the free and the bound state, averaged on time spans of 1 ns.

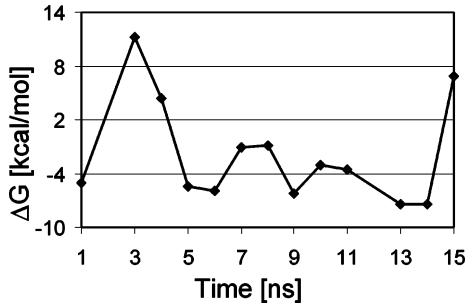

Figure 21. PAM and SX4 free binding energy with IgG evaluated with the LIE protocol (time span of 1 ns).

established between PAM and IgG, but rather that the extent of such interactions is comparable to those with agarose.

4. Conclusions

This paper discusses the computational investigation of the interaction between IgG and ligands supported on agarose by means of molecular dynamics; two commercial ligands, A2P and PAM, were considered. Simulations were started from ligand−protein binding structures determined, either computationally or experimentally, for a non-immobilized ligand; subsequently the complex was covalently bound to agarose through a spacer arm. The conformational evolution of the supported ligand−protein complex was then investigated through MD simulations of 15 ns. The system takes about 5 ns to reach a stable state, which is then maintained for the rest of the simulation except for the PAM ligand, in which case at the end of the simulation a protein macroscopic modification, probably determined by the consideration of only the half FC domain of IgG, starts taking place.

Though much care has been placed in the development of a molecular IgG-ligand-spacer-support model that might mimic as much as possible the real chromatographic material, the molecular model here investigated is in many aspects an ideal system. Two relevant approximations are the consideration of a single IgG subclass with an atomistically defined molecular structure and the consideration of a liquid buffer consistent of pure water, thus neglecting the influence of impurities and the effect of the salt concentration. This means the results here presented should be considered as a limiting case and that deviation from it should be expected when considering real feedstocks. To further our understanding of this system simulations are in progress in order to investigate how a change of the composition of the buffer might influence the material performances.

A detailed energetic analysis of the interaction of the supported ligands with the antibody made it possible to identify and quantify the molecular driving forces responsible for the bond formation. In the case of A2P, the VdW and electrostatic energies of interaction between the ligand-spacer pair and the protein are significant but are of the same magnitude as those of interaction with the support material, so that the net free binding energy is only slightly negative. In the case of PAM, electrostatic energies of interaction of the ligand with protein and support are as well balanced, but van der Waals forces favor the formation of a stable bond with the protein. This can be ascribed to the higher complexity of this ligand whose four arms, each one containing three aminoacids, are only partly involved in the interaction with agarose and are thus free to bind the protein.

The computational results here presented and in particular the quantification of the energies of interaction of the ligand with support and antibody lead us to conclude that the interaction with the support material can indirectly affect the strength of the bond between immobilized affinity chromatography ligands and proteins. This is particularly true for the FC "consensus binding site" of IgG antibodies, as it requires a significant mobility of the ligand in order to be accessed.

Acknowledgment

The authors are grateful to Giorgio Fassina and Paolo Pengo from Xeptagen, Sharon Williams from Prometic Bioscience, and Wolfgang Lindner for continuous and fruitful discussions. We thank the European Commission for funding this work under the integrated project Advanced Interactive Materials by Design (contract NMP3-CT2004-500160).

References and Notes

(1) Waldmann, T. A.; Levy, R.; Coller, B. S. Emerging therapies: Spectrum of applications of monoclonal antibody therapy. *Hematology* **2000**, *2000*, 394−408.
(2) Saphire, E. O.; Parren, P. W. H. I.; Pantophlet, R.; Zwick, M. B.; Morris, G. M.; Rudd, P. M.; Dwek, R. A.; Stanfield, R. L.; Burton, D. R.; Wilson, I. A. Crystal structure of a neutralizing human IgG against HIV-1: A template for vaccine design. *Science* **2001**, *293*, 1155−1159.
(3) Scallon, B. J.; Snyder, L. A.; Anderson, G. M.; Chen, Q. M.; Yan, L.; Weiner, L. M.; Nakada, M. T. A review of antibody therapeutics and antibody-related technologies for oncology. *J. Immunother.* **2006**, *29*, 351−364.
(4) Kim, S. J.; Park, Y.; Hong, H. J. Antibody engineering for the development of therapeutic antibodies. *Mol. Cells* **2005**, *20*, 17−29.
(5) Filpula, D. Antibody engineering and modification technologies. *Biomol. Eng.* **2007**, *24*, 201−215.
(6) Maggon, K. Monoclonal antibody "gold rush". *Curr. Med. Chem.* **2007**, *14*, 1978−1987.
(7) Shukla, A. A.; Hubbard, B.; Tressel, T.; Guhan, S.; Low, D. Downstream processing of monoclonal antibodies−Application of platform approaches. *J. Chromatogr. B* **2007**, *848*, 28−39.
(8) Wurm, F. M. Production of recombinant protein therapeutics in cultivated mammalian cells. *Nat. Biotechnol.* **2004**, *22*, 1393−1398.
(9) Kurtzman, A. L.; Govindarajan, S.; Vahle, K.; Jones, J. T.; Heinrichs, V.; Patten, P. A. Advances in directed protein evolution by recursive genetic recombination: applications to therapeutic proteins. *Curr. Opin. Biotechnol.* **2001**, *12*, 361−370.
(10) Graddis, T. J. R. J. R. L.; McGrew, J. T. Designing proteins that work using recombinant technologies. *Curr. Pharm. Biotechnol.* **2002**, *3*, 285−297.
(11) Keller, K.; Friedmann, T.; Boxman, A. The bioseparation needs for tomorrow. *Trends Biotechnol.* **2001**, *19*, 438−441.
(12) Roque, A. C. A.; Lowe, C. R.; Taipa, M. A. Antibodies and genetically engineered related molecules: Production and purification. *Biotechnol. Prog.* **2004**, *20*, 639−654.
(13) Huse, K. B. H. J.; Scholz, G. H. Purification of antibodies by affinity chromatography. *J. Biochem. Biophys. Methods* **2002**, *51*, 217−231.

(14) Roque, A. C. A.; Silva, C. S. O.; Taipa, M. A. Affinity-based methodologies and ligands for antibody purification: Advances and perspectives. *J. Chromatogr. A* **2007**, *1160*, 44−55.
(15) Hober, S.; Nord, K.; Linhult, M. Protein A chromatography for antibody purification. *J. Chromatogr. B* **2007**, *848*, 40−47.
(16) Kihira, Y.; Aiba, S. Artificial Immunoglobulin G-Binding Protein Mimetic to Staphylococcal Protein-a−Its Production and Application to Affinity Purification of Immunoglobulin-G. *J. Chromatogr.* **1992**, *597*, 277−283.
(17) Fassina, G.; Verdoliva, A.; Odierna, M. R.; Ruvo, M.; Cassini, G. Protein a mimetic peptide ligand for affinity purification of antibodies. *J. Mol. Recognit.* **1996**, *9*, 564−569.
(18) Li, R. X.; Dowd, V.; Stewart, D. J.; Burton, S. J.; Lowe, C. R. Design, synthesis, and application of a Protein A mimetic. *Nat. Biotechnol.* **1998**, *16*, 190−195.
(19) Newcombe, A. R.; Cresswell, C.; Davies, S.; Watson, K.; Harris, G.; O'Donovan, K.; Francis, R. Optimised affinity purification of polyclonal antibodies from hyper immunised ovine serum using a synthetic Protein A adsorbent, MAbsorbento (R) A2P. *J. Chromatogr. B* **2005**, *814*, 209−215.
(20) Clonis, Y. D. Affinity chromatography matures as bioinformatic and combinatorial tools develop. *J. Chromatogr. A* **2006**, *1101*, 1−24.
(21) Fassina, G.; Ruvo, M.; Palombo, G.; Verdoliva, A.; Marino, M. Novel ligands for the affinity-chromatographic purification of antibodies. *J. Biochem. Biophys. Methods* **2001**, *49*, 481−490.
(22) Lowe, C. R. Combinatorial approaches to affinity chromatography. *Curr. Opin. Chem. Biol.* **2001**, *5*, 248−256.
(23) Zhang, X.; Wang, J. C.; Lacki, K. M.; Liapis, A. I. Molecular dynamics simulation studies of the transport and adsorption of a charged macromolecule onto a charged adsorbent solid surface immersed in an electrolytic solution. *J. Colloid Interface Sci.* **2004**, *277*, 483−498.
(24) Zhang, X.; Grimes, B. A.; Wang, J. C.; Lacki, K. M.; Liapis, A. I. Analysis and parametric sensitivity of the behavior of overshoots in the concentration of a charged adsorbate in the adsorbed phase of charged adsorbent particles: practical implications for separations of charged solutes. *J. Colloid Interface Sci.* **2004**, *273*, 22−38.
(25) Busini, V.; Moiani, D.; Moscatelli, D.; Zamolo, L.; Cavallotti, C. Investigation of the influence of spacer arm on the structural evolution of affinity ligands supported on agarose. *J. Phys. Chem. B* **2006**, *110*, 23564−23577.
(26) DeLano, W. L.; Ultsch, M. H.; de Vos, A. M.; Wells, J. A. Convergent solutions to binding at a protein-protein interface. *Science* **2000**, *287*, 1279−1283.
(27) Dinon, F.; Fassina, G. Personal communication, 2006, Xeptagen, Italy.
(28) Fassina, G.; Verdoliva, A.; Palombo, G.; Ruvo, M.; Cassani, G. Immunoglobulin specificity of TG19318: a novel synthetic ligand for antibody affinity purification. *J. Mol. Recognit.* **1998**, *11*, 128−133.
(29) Cornell, W. D.; Cieplak, P.; Bayly, C. I.; Gould, I. R.; Merz, K. M., Jr.; Ferguson, D. M.; Spellmeyer, D. C.; Fox, T.; Caldwell, J. W.; Kollman, P. A. A second generation force field for the simulation of proteins, nucleic acids, and organic molecules. *J. Am. Chem. Soc.* **1995**, *117*, 5179.
(30) Bujacz, G. D. Personal Communication, 2006, Technical University of Lodz, Poland.
(31) Deisenhofer, J. Crystallographic refinement and atomic models of a human Fc fragment and its complex with fragment B of Protein A from *Staphylococcus aureus* at 2.9- and 2.8-Å Resolution. *Biochemistry* **1981**, *20*, 2361−2370.
(32) Case, D. A.; Darden, T. A.; Cheatham, T. E., III; Simmerling, C. L.; Wang, J.; Duke, R. E.; Luo, R.; Merz, K. M.; Wang, B.; Pearlman, D. A.; Crowley, M.; Brozell, S.; Tsui, H.; Gohlke, H.; Mongan, J.; Hornak, V.; Cui, G.; Beroza, P.; Schafmeister, C.; Caldwell, J. W.; Ross, W. S.; Kollman, P. A. AMBER 8, 8.0; University of California, San Francisco, 2004.
(33) Kirschner, K. N.; Woods, R. J. Solvent interactions determine carbohydrate conformation. *Proc. Natl. Acad. Sci. U.S.A.* **2001**, *98*, 10541−10545.
(34) Kirschner, K. N.; Woods, R. J. Quantum mechanical study of the nonbonded forces in water-methanol complexes. *J. Phys. Chem. A* **2001**, *105*, 4150−4155.
(35) Basma, M.; Sundara, S.; Calgan, D.; Vernali, T.; Woods, R. J. Solvated ensemble averaging in the calculation of partial atomic charges. *J. Comput. Chem.* **2001**, *22*, 1125−1137.
(36) Parr, R. G.; Yang, W. *Density-Functional Theory of Atoms and Molecules*; Oxford University Press: New York, 1989.
(37) Lee, C.; Yang, W.; Parr, R. G. Development of the Colle-Salvetti correlation-energy formula into a functional of the electron density. *Phys. Rev. B* **1988**, *37*, 785.
(38) Becke, A. D. Density-functional thermochemistry. III. The role of exact exchange. *J. Chem. Phys.* **1993**, *98*, 5648−5652.
(39) Stephens, P. J.; Devlin, F. J.; Chabalowski, C. F.; Frisch, M. J. Ab initio calculation of vibrational absorption and circular dichroism spectra using density functional force fields. *J. Phys. Chem.* **1994**, *98*, 11623−11627.
(40) Bayly, C. I.; Cieplak, P.; Cornell, W. D.; Kollman, P. A. A Well-behaved electrostatic potential based method using charge restraints for deriving atomic charges. The Resp Model. *J. Phys. Chem.* **1993**, *97*, 10269.
(41) Case, D. A.; Cheatham, T. E.; Darden, T.; Gohlke, H.; Luo, R.; Merz, K. M.; Onufriev, A.; Simmerling, C.; Wang, B.; Woods, R. J. The Amber biomolecular simulation programs. *J. Comput. Chem.* **2005**, *26*, 1668−1688.
(42) Ryckaert, J. P.; Ciccotti, G.; Berendsen, H. J. C. Numerical integration of the Cartesian equations of motion of a system with constrains: molecular dynamics of *n*-alkanes. *J. Comput. Phys.* **1977**, *23*, 327−341.
(43) Baker, N. A. Improving implicit solvent simulations: a Poisson-centric view. *Curr. Opin. Struct. Biol.* **2005**, *15*, 137−143.
(44) Feig, M.; Brooks, C. L. Recent advances in the development and application of implicit solvent models in biomolecule simulations. *Curr. Opin. Struct. Biol.* **2004**, *14*, 217−224.
(45) Eisenberg, D.; McLachlan, A. D. Solvation energy in protein folding and binding. *Nature* **1986**, *319*, 199−203.
(46) Wesson, L.; Eisenberg, D. Atomic solvation parameters applied to molecular dynamics of proteins in solution. *Protein Sci.* **1992**, *1*, 227−235.
(47) Carlsson, J.; Ander, M.; Nervall, M.; Aqvist, J. Continuum solvation models in the linear interaction energy method. *J. Phys. Chem. B* **2006**, *110*, 12034−12041.
(48) Aqvist, J.; Hansson, T. On the validity of electrostatic linear response in polar solvents. *J. Phys. Chem.* **1996**, *100*, 9512−9521.
(49) Blokzijl, W.; Engberts, J. Hydrophobic effects. Opinions and facts. *Angew. Chem., Int. Ed. Engl.* **1993**, *32*, 1545−1579.
(50) Aqvist, J.; Medina, C.; Samuelsson, J. E. New method for predicting binding-affinity in computer-aided drug design. *Protein Eng.* **1994**, *7*, 385−391.
(51) Frisch, M. J.; Trucks, G. W.; Schlegel, H. B.; Scuseria, G. E.; Robb, M. A.; Cheeseman, J. R.; Montgomery, J. A.; Jr., T. V.; Kudin, K. N.; Burant, J. C.; Millam, J. M.; Iyengar, S. S.; Tomasi, J.; Barone, V.; Mennucci, B.; Cossi, M.; Scalmani, G.; Rega, N.; Petersson, G. A.; Nakatsuji, H.; Hada, M.; Ehara, M.; Toyota, K.; Fukuda, R.; Hasegawa, J.; Ishida, M.; Nakajima, T.; Honda, Y.; Kitao, O.; Nakai, H.; Klene, M.; Li, X.; Knox, J. E.; Hratchian, H. P.; Cross, J. B.; Bakken, V.; Adamo, C.; Jaramillo, J.; Gomperts, R.; Stratmann, R. E.; Yazyev, O.; Austin, A. J.; Cammi, R.; Pomelli, C.; Ochtersk, J. W.; Ayala, P. Y.; Morokuma, K.; Voth, G. A.; Salvador, P.; Dannenberg, J. J.; Zakrzewski, V. G.; Dapprich, S.; Daniels, A. D.; Strain, M. C.; Farkas, O.; Malick, D. K.; Rabuck, A. D.; Raghavachari, K.; Foresman, J. B.; Ortiz, J. V.; Cui, Q.; Baboul, A. G.; Clifford, S.; Cioslowski, J.; Stefanov, B. B.; G. Liu, A. L.; Piskorz, P.; Komaromi, I.; Martin, R. L.; Fox, D. J.; Keith, T.; Al-Laham, M. A.; Peng, C. Y.; Nanayakkara, A.; Challacombe, M.; Gill, P. M. W.; Johnson, B.; Chen, W.; Wong, M. W.; Gonzalez, C.; Pople, J. A. *Gaussian 03*, Revision C.01; Gaussian Inc.: Pittsburgh, 2003.
(52) Schaftenaar, G.; Noordik, J. H. Molden: a pre- and post-processing program for molecular and electronic structures. *J. Comput.-Aided Mol. Des.* **2000**, *14*, 123−134.
(53) Humphrey, W.; Dalke, A.; Schulten, K. VMD: Visual molecular dynamics. *J. Mol. Graphics* **1996**, *14*, 33−38.
(54) Morris, G. M.; Goodsell, D. S.; Halliday, R. S.; Huey, R.; Hart, W. E.; Belew, R. K.; Olson, A. J. Automated docking using a

Lamarckian genetic algorithm and an empirical binding free energy function. *J. Comput. Chem.* **1998**, *19*, 1639−1662.
(55) Arnott, S.; Fulmer, A.; Scott, W. E.; Dea, I. C. M.; Moorhouse, R.; Rees, D. A. The agarose double helix and its function in agarose gel structure. *J. Mol. Biol.* **1974**, *90*, 269.
(56) Ramzi, M.; Rochas, C.; Guenet, J. M. Phase behavior of agarose in binary solvents. *Macromolecules* **1996**, *29*, 4668−4674.
(57) Ramzi, M.; Rochas, C.; Guenet, J. M. Structure-properties relation for agarose thermoreversible gels in binary solvents. *Macromolecules* **1998**, *31*, 6106−6111.
(58) Xiong, J. Y.; Narayanan, J.; Liu, X. Y.; Chong, T. K.; Chen, S. B.; Chung, T. S. Topology evolution and gelation mechanism of agarose gel. *J. Phys. Chem. B* **2005**, *109*, 5638−5643.
(59) Moiani, D.; Salvalaglio, M.; Cavallotti, C.; Bujacz, G. D.; Dinon, F.; Pengo, P.; Fassina, G. A Protein-A mimetic peptide dendrimer binds to human IgG. Manuscript in preparation.

Received November 30, 2007. Accepted April 3, 2008.

BP070469Z